Non-Precious Metal Nitrides for Efficient Electrochemical Water Splitting

by

Yufeng Chen

Department of Chemistry
Duke University

Defense Date: July 11, 2025

Approved:

Jie Liu, Advisor

Stephen L. Craig

Jeffrey T. Glass

Michael J. Therien

Thesis submitted in partial fulfillment of the requirements for the degree of Master of Science in the Department of Chemistry in The Graduate School of
Duke University
2025

ABSTRACT

Non-Precious Metal Nitrides for Efficient Electrochemical Water Splitting
by

Yufeng Chen

Department of Chemistry
Duke University

Defense Date: July 11, 2025

Approved:

Jie Liu, Advisor

Stephen L. Craig

Jeffrey T. Glass

Michael J. Therien

An abstract of a thesis submitted in partial fulfillment of the requirements for the degree of
Master of Science in the Department of Chemistry in The Graduate School of
Duke University
2025

Abstract

Growing global energy demands coupled with the detrimental environmental impacts of fossil fuel combustion highlight an urgent need to develop sustainable energy technologies. Electrochemical water splitting stands as a promising approach to convert renewable energy sources to hydrogen, a clean and carbon free energy carrier, for applications and energy transportation. However, the process requires efficient, durable, and cost-effective electrocatalysts that are still being developed. Non-precious metal nitrides have recently garnered significant attention due to their excellent catalytic properties, low cost, and high stability. This thesis focuses on several important aspects related to this catalyst family. Chapter 1 discusses recent advancements and fundamental methodologies in electrocatalyst research relevant to water splitting applications. Chapter 2 describes the system involving the development of nitridated $NiMoO_4$ nanoneedles as a catalyst for the hydrogen evolution reaction (HER). The optimized material shows strong HER performance in alkaline solution, with low overpotentials, favorable Tafel slopes, and stable long-term operation. Notably, the catalyst reaches a high current density of 350 mA/cm^2 at an overpotential of only -10 mV, showing its potential for practical hydrogen production. Chapter 3 focuses on Co_3Mo_3N nanoparticles used as a photo-thermal electrocatalyst for the oxygen evolution reaction (OER) and its improved performance under both light and heat. Electrochemical testing shows that Co_3Mo_3N catalyst has a significant photo-thermal enhancement in OER. For example, under 2 watts of blue light, it achieves a 150% increase in current density at an overpotential of 0.34 V. The outstanding effect of photo-thermal enhancement of the catalyst indicates its potential in light-assisted water-splitting technologies. Overall, this research supports the development of affordable, high-performance catalytic materials for clean energy applications.

Contents

List of Figures

Chapter 1: Introduction

1.1 Global energy challenges and the desire for sustainable, clean energy sources

The 21st century confronts humanity with one of its most urgent and complex challenges: meeting the growing global demand for energy while mitigating climate change and reducing environmental degradation. Energy underpins nearly every aspect of human development, including powering industrial processes, transportation networks, health systems, and digital infrastructure. However, the global energy supply remains heavily reliant on fossil fuels (coal, oil, and natural gas), which together accounted for over 80% of primary energy consumption as of 2022[1]. This dependence poses serious threats to environmental sustainability, energy security, and socioeconomic stability.

Fossil fuel combustion is the primary driver of anthropogenic greenhouse gas (GHG) emissions, responsible for more than 75% of global CO_2 output[2]. The accumulation of GHGs in the atmosphere has led to rising global temperatures, melting polar ice, sea-level rise, and an increase in the frequency and intensity of extreme weather events. The Intergovernmental Panel on Climate Change (IPCC) warns that global warming must be limited to 1.5 °C above pre-industrial levels to avoid catastrophic and potentially irreversible climate impacts. Achieving this target requires halving global CO_2 emissions by 2030 and reaching net-zero by 2050[3].

In addition to environmental degradation, fossil fuel exploitation is associated with local air and water pollution, land use conflicts, and resource-driven geopolitical tensions. The uneven geographical distribution of hydrocarbon reserves has contributed to price volatility, trade imbalances, and energy insecurity in import-dependent nations[4]. Meanwhile, driven by population expansion, urbanization, and rising living standards, global energy demand continues to grow, particularly in emerging economies. According to projections by the International Energy Agency (IEA), global energy consumption will increase by approximately 25% by 2040 under stated policy scenarios[5]. Meeting this demand using conventional fossil-based infrastructure would render international climate goals unattainable.

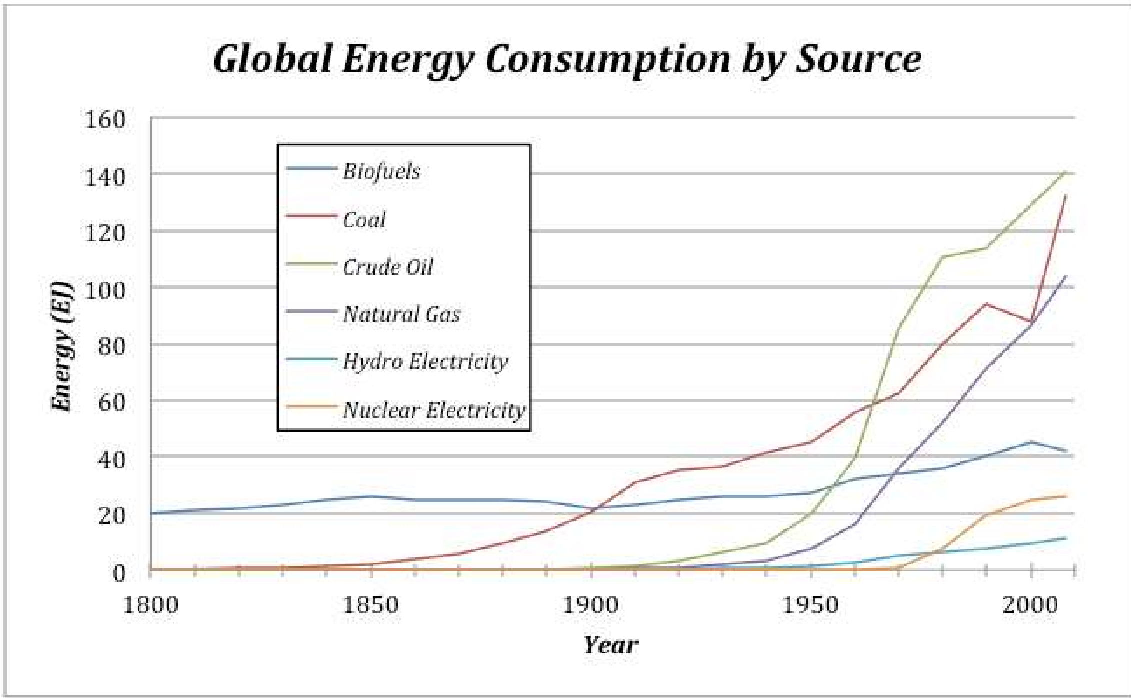

Figure 1.1 Global energy consumption by source, 1800-2000[6].

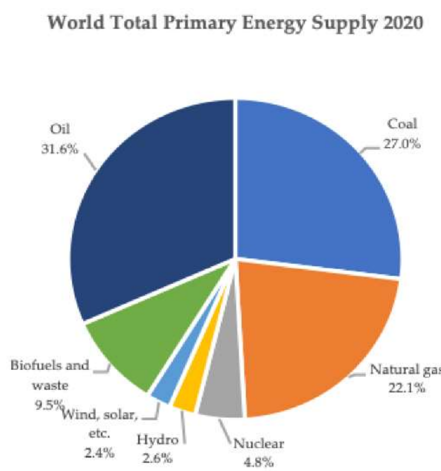

Figure 1.2 World Total Primary Energy Supply by Source.

To address this pressing challenge, the international community has begun a transition toward sustainable and clean energy systems. Clean energy refers to energy generated from low-or zero-emission sources, including solar, wind, hydroelectric, geothermal, biomass, and nuclear energy. Sustainable energy, more broadly, encompasses the principles of environmental responsibility, economic viability, and social equity. The deployment of renewable energy technologies has accelerated in recent years, with solar and wind power reaching cost parity with or even outperforming fossil fuels in many regions[8]. Nevertheless, these sources face challenges related to intermittency, variability, and infrastructure compatibility.

A core enabler of the clean energy transition is innovation in energy conversion and storage technologies. Electrochemical systems, such as batteries, fuel cells, and water electrolyzers, play a pivotal role in decoupling energy generation from demand by enabling the storage of renewable electricity and the production of green fuels. In particular, hydrogen produced via water electrolysis using renewable power, often referred to as “green hydrogen”, offers a promising route to decarbonize energy-intensive sectors that are difficult to electrify directly, such as heavy industry and long-distance transportation[9].

Realizing the potential of such technologies requires addressing several persistent challenges, including high material costs, low catalytic efficiency, and limited durability of current energy materials. For example, state-of-the-art electrolyzers rely on platinum group metals (PGMs) like Pt, Ir, and Ru, which are scarce and expensive. This has prompted a surge in research into earth-abundant alternatives, including transition metal compounds such as oxides, phosphides, carbides, and nitrides[10]. Progress in these areas hinges on advancements in materials synthesis, interface engineering, and mechanistic understanding at the atomic level.

1.2 Hydrogen: a clean energy carrier

As the global community strives to mitigate the impacts of climate change and achieve carbon neutrality, hydrogen has emerged as a pivotal clean energy carrier capable of transforming the energy landscape. With the accelerating deployment of renewable energy technologies and the growing urgency to decarbonize hard-to-abate sectors, hydrogen offers a flexible, scalable, and environmentally benign solution to several critical energy challenges. Unlike traditional fossil fuels, hydrogen can be produced from a wide range of feedstocks, used across diverse applications, and generates no greenhouse gas emissions at the point of use, making it an ideal complement to renewable electricity in the transition toward sustainable energy systems.

Hydrogen is the most abundant element in the universe, and hydrogen gas possesses a high gravimetric energy density of approximately 120 MJ kg^{-1}, which is nearly three times that of gasoline. When used in a fuel cell or combusted, hydrogen reacts with oxygen to form water, releasing energy without emitting carbon dioxide or other pollutants. These attributes make hydrogen particularly attractive for use in fuel cell electric vehicles, stationary power systems, and industrial processes. Moreover, hydrogen can be stored in gaseous or liquid form and transported via pipelines, road tankers, or chemical carriers such as ammonia and methanol, enabling long-duration and cross-regional energy storage and trade[11].

A key feature of hydrogen as an energy carrier is its ability to bridge the temporal and spatial gaps inherent in renewable energy systems. Solar and wind energy, while environmentally sustainable, suffer from intermittency and geographic limitations. Hydrogen, produced via electrolysis using surplus renewable electricity, can act as a chemical battery, storing energy for later use or transport. This capability is essential for grid balancing, seasonal storage, and integrating variable renewable sources into national and regional energy systems[12].

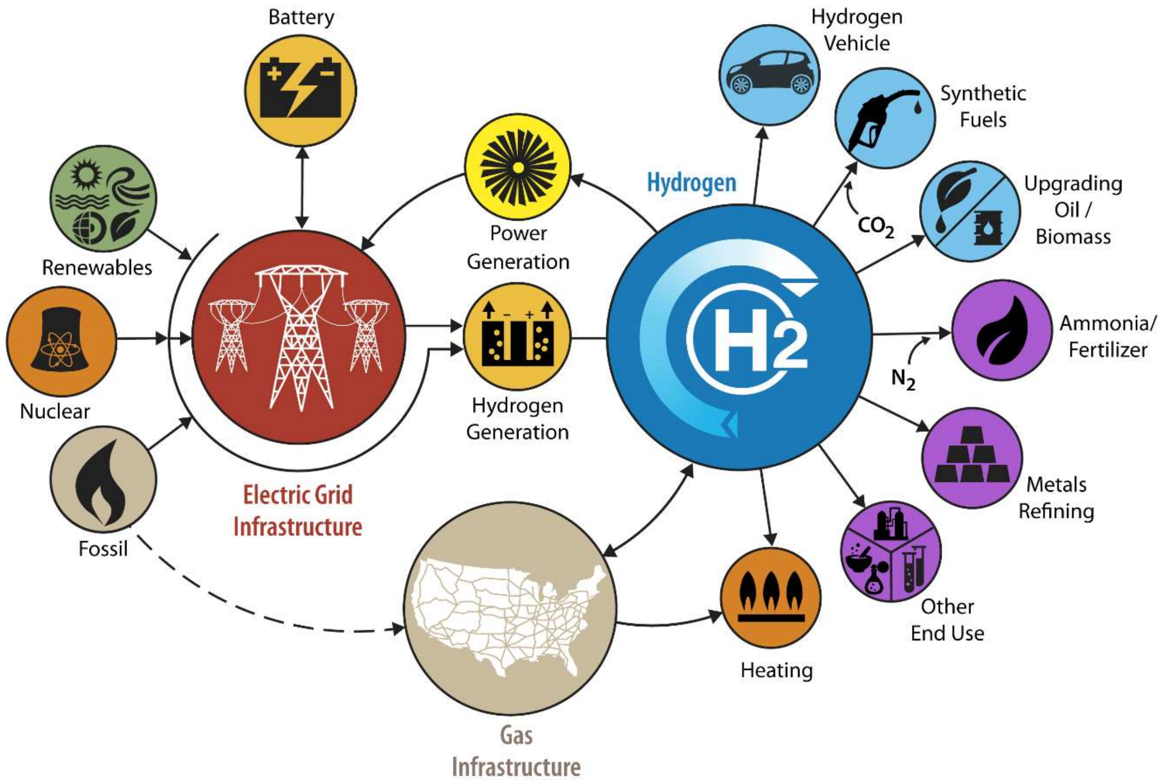

Figure 1.3 Hydrogen value chain linking power, gas infrastructure, and end uses[13].

The environmental profile of hydrogen depends strongly on the production pathway. Conventionally, over 95% of hydrogen is produced from fossil fuels, primarily through steam methane reforming (SMR) of natural gas, without carbon capture, resulting in significant CO_2 emissions. This form is referred to as “grey hydrogen”. “Blue hydrogen” uses similar processes but incorporates carbon capture, utilization, and storage technologies to reduce emissions. “Green hydrogen”, the most sustainable form, is generated by water electrolysis powered by renewable electricity, resulting in near-zero carbon emissions throughout the production cycle[12]. Although green hydrogen is currently more expensive than grey or blue alternatives, declining renewable electricity costs and improvements in electrolyzer technology are expected to reduce its cost significantly in the coming decade.

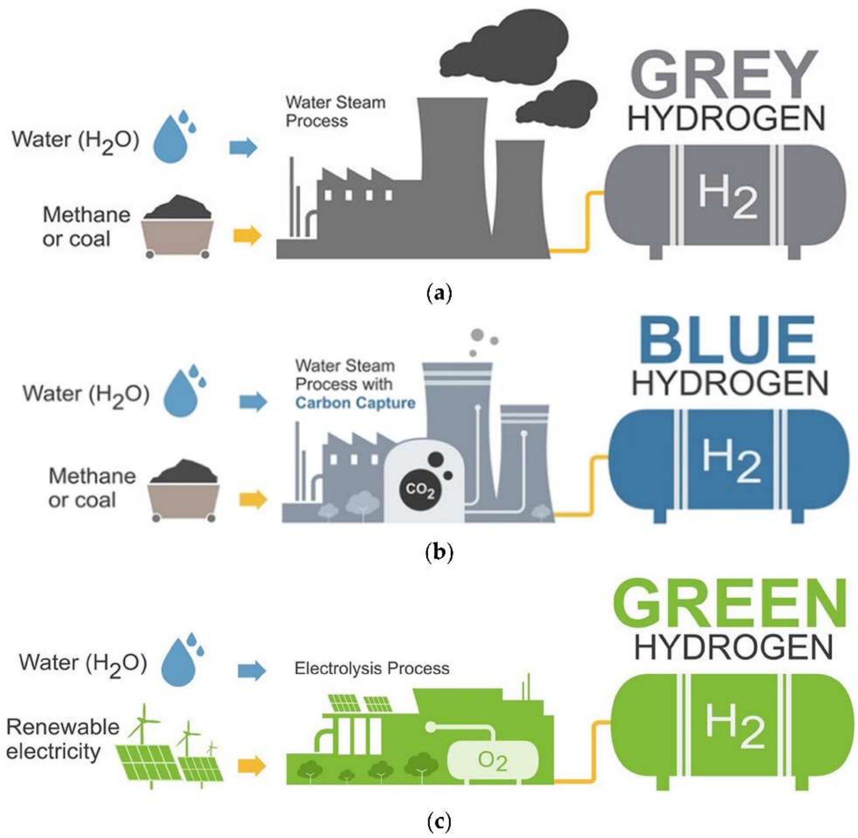

Figure 1.4 Type of hydrogen production.

This figure is adapted with permission from reference[14]. Licensed under CC BY 4.0 https://creativecommons.org/licenses/by/4.0/

Hydrogen is also uniquely positioned to support decarbonization across a wide array of sectors. In the power sector, it can serve as a dispatchable energy reserve for renewable-dominated grids, offering medium- to long-term storage options that batteries cannot economically provide. In transportation, hydrogen fuel cell technology is particularly well-suited for heavy-duty applications, such as freight trucks, buses, trains, and marine vessels, where battery systems face limitations in range, weight, and refueling time[15]. In industrial applications, hydrogen is already used as a feedstock in the production of ammonia and methanol and is being explored as a substitute for coking coal in low-emission steelmaking via the direct reduction of iron process. Furthermore, blending hydrogen into natural gas pipelines for residential and commercial heating is being piloted in several countries, although compatibility and safety concerns remain.

The strategic importance of hydrogen is increasingly reflected in national and regional policy frameworks. Numerous countries have launched dedicated hydrogen strategies that outline roadmaps for production, infrastructure development, and market creation. For example, the European Commission's 2020 hydrogen strategy sets a target of 40 GW of electrolyzer capacity by 2030 and supports the development of hydrogen valleys across member states[4]. In the United States, the Department of Energy's Hydrogen Energy Earthshot aims to reduce the cost of clean hydrogen to $1/kg within a decade[9].

Despite its promise, widespread adoption of hydrogen faces several scientific, technical, and economic barriers. High production costs, especially for green hydrogen, limited hydrogen infrastructure, and challenges related to storage, safety, and materials compatibility remain key obstacles.

1.3 Fundamentals of electrochemical water splitting in hydrogen production

Electrochemical water splitting (EWS) is a foundational reaction for the sustainable production of hydrogen, offering a clean method to store renewable electricity in the form of chemical energy. By decomposing water into hydrogen and oxygen under the influence of an external electric current, this process supports the global push toward carbon neutrality. A rigorous understanding of its thermodynamic, kinetic, and electrochemical fundamentals is essential for advancing water-splitting technologies and optimizing their efficiency in practical applications[16].

The water splitting process involves the overall reaction:

$$\mathrm{H_2O\ (l)} \rightarrow \mathrm{H_2\ (g)} + \frac{1}{2}\mathrm{O_2\ (g)}$$

This reaction has a standard Gibbs free energy change ($\Delta G°$) of +237.2 kJ mol^{-1}, which corresponds to a minimum thermodynamic cell voltage of 1.23 V at 25 °C under standard conditions. However, in real systems, additional voltage, termed overpotential, is required to overcome kinetic barriers and system losses, raising the operational cell voltage to typically between 1.5 and 1.8 V[17].

Electrochemical water splitting is composed of two half-reactions: the hydrogen evolution reaction (HER) at the cathode and the oxygen evolution reaction (OER) at the anode. The nature of these reactions varies depending on the pH of the electrolyte. In acidic media, HER proceeds via the reduction of protons:

$$2H^+ + 2e^- \rightarrow H_2$$

while the corresponding OER involves:

$$H_2O \rightarrow \frac{1}{2}O_2 + 2H^+ + 2e^-$$

In alkaline media, the HER occurs via water reduction:

$$2H_2O + 2e^- \rightarrow H_2 + 2OH^-$$

and the OER is:

$$4OH^- \rightarrow O_2 + 2H_2O + 4e^-$$

Despite its simplicity on paper, HER follows a multi-step mechanism typically initiated by the Volmer step (electrochemical adsorption of hydrogen atoms onto the catalyst surface). This is followed either by the Heyrovsky step (electrochemical desorption) or the Tafel step (chemical recombination of adsorbed hydrogen atoms), depending on the surface properties and electrolyte environment[18]. In alkaline electrolytes, the initial water dissociation required for proton generation adds an additional kinetic barrier to HER, making it slower than in acidic environments[19].

OER is thermodynamically uphill and kinetically sluggish due to its four-electron nature and multiple adsorbed intermediates, such as OH^*, O^*, and OOH^*. The formation of the O-O bond and desorption of molecular oxygen from the catalyst surface represent the key challenges. These steps necessitate high overpotentials, often exceeding 300-500 mV, even with state-of-the-art catalysts[10].

A typical electrolysis cell consists of an anode and a cathode separated by an electrolyte (either liquid or solid) and may include a membrane or diaphragm to prevent the mixing of hydrogen and oxygen gases. There are four primary types of water electrolyzers. Proton exchange membrane water electrolyzer (PEMWE) employs a solid polymer electrolyte that conducts protons and operates under acidic conditions, offering high current densities and compact system design. Anion exchange membrane water electrolyzer (AEMWE) utilizes a hydroxide-conducting anion exchange membrane and alkaline-compatible catalysts, enabling low-cost, noble-metal-free operation. Alkaline water electrolyzer (AWE) is a mature technology that uses a liquid alkaline electrolyte (typically KOH) and porous diaphragm, with stable, low-cost catalysts and moderate efficiency. Solid oxide electrolyzer (SOE) operates at high temperatures (>700 °C) using a ceramic oxide electrolyte to transport oxygen ions, achieving high efficiency through thermal-electrochemical synergy.

To better understand water splitting at the molecular and device levels, performance metrics are often used to assess catalyst and system behavior. The overpotential (η) quantifies the additional driving force required beyond the thermodynamic minimum. The Tafel slope provides mechanistic insight by indicating how the current density varies with applied voltage. The exchange current density (j_0) reflects the intrinsic activity of a material at equilibrium, while the Faradaic efficiency represents the proportion of current that contributes directly to product formation. Finally, stability over extended operation is essential for practical application[20].

The performance of water splitting is fundamentally constrained by the sluggish kinetics of the OER, particularly under neutral or alkaline conditions, where water must first dissociate to release reactive species. This inherent asymmetry between the HER and OER has prompted intensive research into electrocatalyst design and reactor engineering.

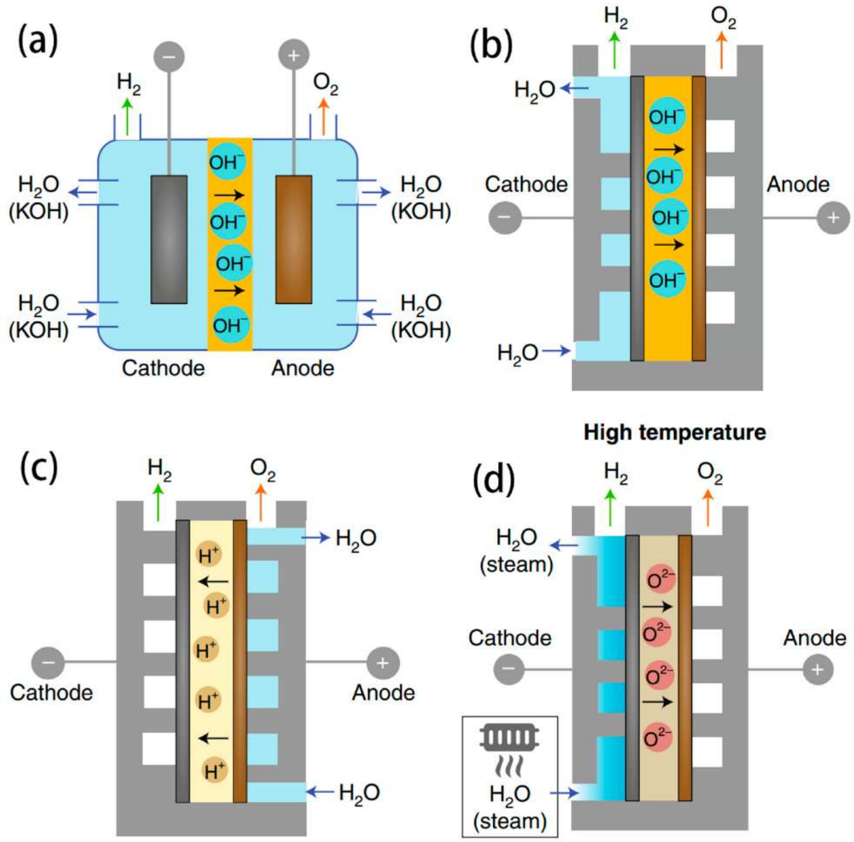

Figure 1.5 Configurations for water electrolysis.

(a) Alkaline water electrolysis (AWE) electrolyser; (b) anion exchange membrane water electrolysis (AEMWE) electrolyser; (c) proton exchange membrane water electrolysis (PEMWE) electrolyser; (d) solid oxide electrolysis cell (SEOC). This figure is adapted with permission from reference[21]. Licensed under CC BY 4.0 https://creativecommons.org/licenses/by/4.0/

1.4 Current progress in electrochemical water splitting

EWS has emerged as a promising strategy for sustainable hydrogen production. However, the wide-scale deployment of this technology remains constrained by the limitations of existing electrocatalyst materials, particularly those based on precious metals. Efficient water splitting requires robust, highly active catalysts that can accelerate both HER and OER while operating under practical conditions. To address the economic and scalability challenges associated with noble metals, significant research has been devoted to the development of earth-abundant transition metal compounds as alternative catalysts.

The state-of-the-art catalysts for HER and OER are currently based on platinum-group metals (PGMs). For HER, platinum is considered the benchmark catalyst due to its optimal hydrogen adsorption energy, low overpotential, and excellent kinetics across both acidic and alkaline media[19]. For OER, iridium and ruthenium oxides exhibit exceptional activity, particularly in acidic environments, where many non-noble metal catalysts tend to degrade rapidly[20]. These materials are capable of achieving low Tafel slopes, high current densities, and long-term operational stability. However, the extreme scarcity, high cost, and geopolitical concentration of PGMs present major obstacles to their widespread commercial application[16].

The high price volatility and limited global reserves of Pt, Ir, and Ru significantly increase the capital costs of electrolyzer systems, particularly proton exchange membrane (PEM) electrolyzers that require noble metals to operate under acidic conditions. Moreover, the sustainability of sourcing and recycling these metals raises environmental and ethical concerns. These limitations have catalyzed a major shift in electrocatalysis research toward the exploration of alternative materials that are more abundant, cost-effective, and structurally versatile.

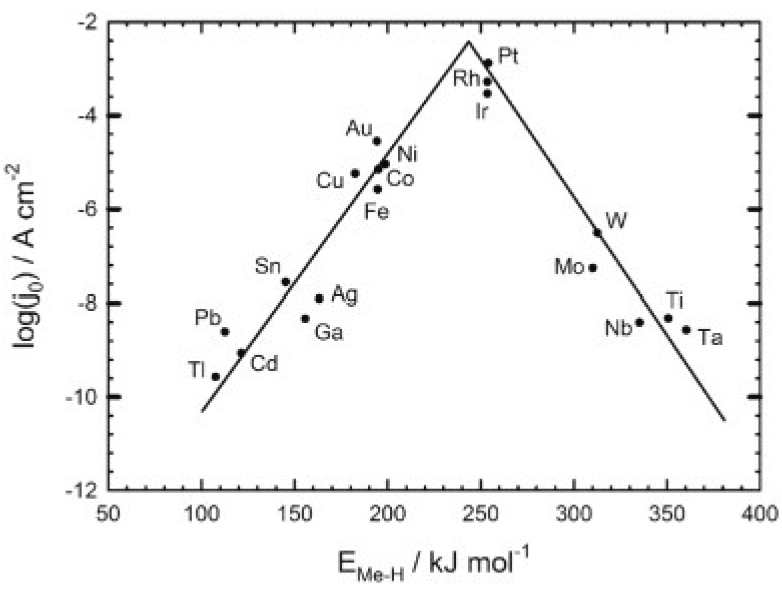

Figure 1.6 HER volcano plot for metals.

This figure is adapted with permission from reference[22]. Licensed under CC BY 4.0 https://creativecommons.org/licenses/by/4.0/

Among the most promising candidates are transition metal-based compounds, which include oxides, sulfides, phosphides, and nitrides. These materials offer diverse crystal structures, adjustable electronic properties, and catalytic tunability through compositional and morphological engineering. Many of these compounds are derived from elements such as iron (Fe), cobalt (Co), nickel (Ni), and molybdenum (Mo), which are orders of magnitude more abundant and economical than PGMs.

Transition metal oxides, especially mixed metal oxides and perovskite-type structures, have shown substantial OER activity in alkaline media[23]. For example, NiFe layered double hydroxides (LDHs) and spinel oxides like Co_3O_4 are widely studied for their high intrinsic activity and stability in basic electrolytes. Their performance can be enhanced further through doping, strain engineering, and interface modification. However, metal oxides generally suffer from poor electrical conductivity, which limits their performance at high current densities without conductive supports[24].

Transition metal sulfides such as MoS_2 and CoS_x have been extensively investigated for HER due to their favorable hydrogen binding energies. In particular, MoS_2 has a layered structure with catalytically active edge sites that can be tailored via defect engineering and heterostructure formation[25]. However, sulfides may undergo phase transformation or leaching under oxidative conditions, limiting their dual-functionality for both HER and OER.

Transition metal phosphides such as Ni_2P, CoP, and FeP have attracted attention as bifunctional catalysts capable of catalyzing both HER and OER with good activity and durability[26]. Their metallic nature endows them with excellent conductivity, while surface phosphorus can modulate the electronic environment of active metal centers. Furthermore, surface oxidation of phosphides during operation may result in the formation of catalytically active oxide/phosphate layers, which contribute to their enhanced OER performance.

Transition metal nitrides represent another promising class of materials that combine high electrical conductivity with robust structural stability. Compounds such as MoN, VN, and Ni_3N have shown considerable promise for HER in both acidic and alkaline media. Their metallic bonding character facilitates fast charge transfer, while the strong metal-nitrogen interactions enable good corrosion resistance and thermal stability[27]. In addition, nitrides exhibit tunable electronic structures that can be engineered to optimize intermediate adsorption and catalytic kinetics.

However, despite these advancements, several challenges remain. Many non-noble metal catalysts show poor stability in acidic electrolytes, which limits their integration into PEM electrolyzers. In addition, achieving bifunctional performance for both HER and OER in a single material remains difficult due to the inherently different electronic requirements of the two half-reactions. To overcome these issues, hybrid materials, surface reconstructions, heteroatom doping, and nanostructuring techniques are increasingly employed to enhance activity, durability, and selectivity.

1.5 Plasmonic and photo-thermal electrocatalysts in water splitting

Recent advances in electrochemical water splitting have extended beyond conventional catalytic design toward the integration of light-matter interactions to enhance catalytic activity. Among emerging strategies, plasmonic and photo-thermal electrocatalysis have gained considerable attention for their potential to improve reaction kinetics and reduce energy input by utilizing light energy to modulate surface reactivity. These hybrid approaches leverage physical phenomena such as localized surface plasmon resonance (LSPR) and photothermal conversion to enable more efficient and tunable electrocatalytic systems.

Plasmonic electrocatalysis involves the excitation of collective oscillations of conduction electrons (plasmons) in nanostructured metals when irradiated with visible or near-infrared light. This resonance leads to enhanced electromagnetic fields localized near the nanoparticle surface and can generate energetic, or “hot” electrons and holes. These energetic carriers can transfer to adjacent adsorbates or semiconductor supports, modulating charge transfer steps in catalytic processes[28]. Gold, silver and copper are typical plasmonic materials owing to their strong LSPR in the visible range.

When incorporated into electrocatalysts, plasmonic nanoparticles can boost water-splitting reactions via several mechanisms[29]. In hot carrier injection mechanism, excited electrons can directly populate the conduction band of a catalyst or reduce adsorbed species such as protons or water molecules. In photothermal heating mechanism, non-radiative decay of plasmons generates localized heat, which can raise the surface temperature of the catalyst and improve reaction kinetics.

These mechanisms can operate individually or synergistically, depending on the material system and illumination conditions. In particular, hybrid systems comprising plasmonic metals integrated with transition metal oxides, nitrides, or chalcogenides have shown promising results in enhancing HER and OER rates under light-assisted electrolysis.

For example, Au-decorated TiO_2 or MoS_2 electrodes have demonstrated enhanced HER activity under visible light due to hot electron injection from plasmonic Au nanoparticles[30]. Similarly, Ag-NiFe LDH hybrids have shown improved OER performance attributed to photothermal heating and enhanced charge separation[31]. These enhancements are especially valuable under mild overpotentials, where traditional catalysts may suffer from sluggish kinetics.

In parallel, photo-thermal electrocatalysis offers an alternative yet complementary mechanism of catalytic enhancement. Here, photothermal materials absorb light and convert it into heat through non-radiative processes. The resulting localized heating at the electrode-electrolyte interface can significantly reduce activation barriers for water-splitting reactions and increase the rate of mass and charge transfer.

Unlike plasmonic effects, which rely on coherent electron oscillations, photothermal effects are more broadly applicable across a wider range of light-absorbing materials, including black phosphorus, carbon-based nanostructures, and wide-bandgap semiconductors with engineered defect states. In these systems, light absorption induces a modest temperature rise (typically tens of degrees Celsius), which can shift the Nernst potential, enhance reaction kinetics, and facilitate gas bubble detachment from the electrode surface[32].

A notable advantage of photothermal strategies is that they do not require external bias modifications or expensive noble metals. For instance, carbon black or carbon nanotube-coated electrodes can generate measurable photothermal enhancements in HER and OER under simulated solar irradiation[33]. Additionally, photothermal heating has been shown to activate otherwise inert catalysts or stabilize metastable surface phases that are more catalytically active.

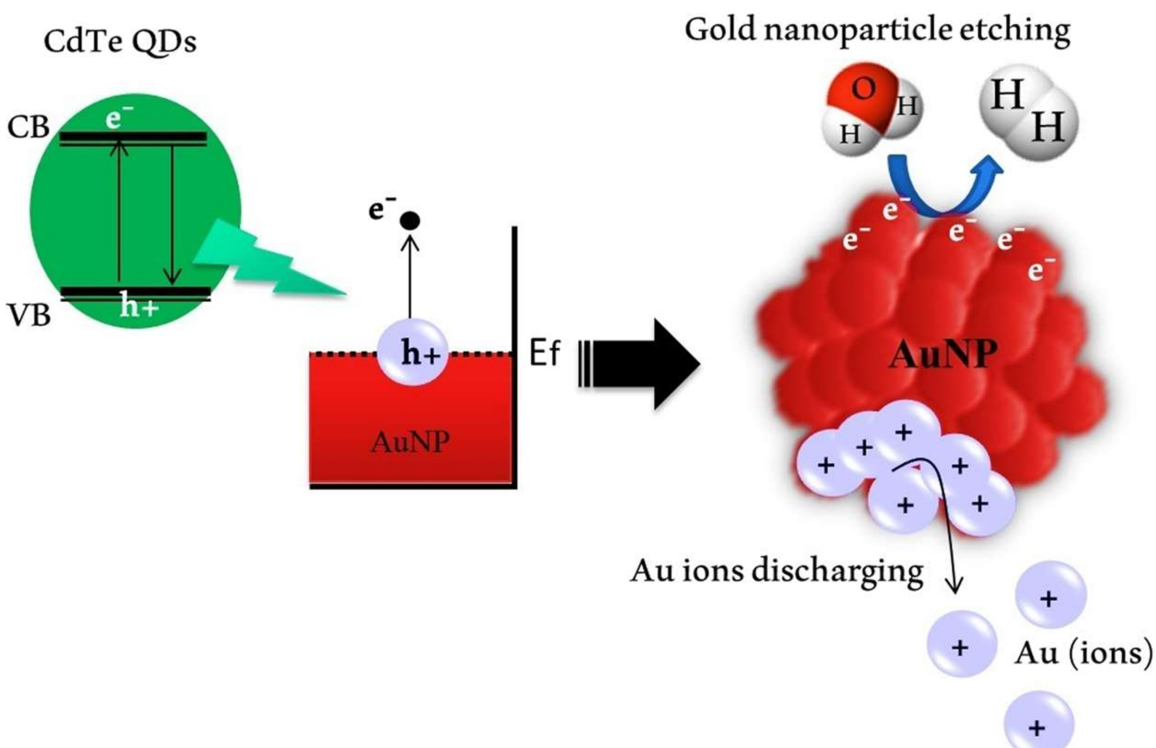

Figure 1.7 Mechanism of dissolution plasmonic AuNPs with water splitting via hot-electron injection by using CdTe QDs photoinduction.

This figure is adapted with permission from reference[34].

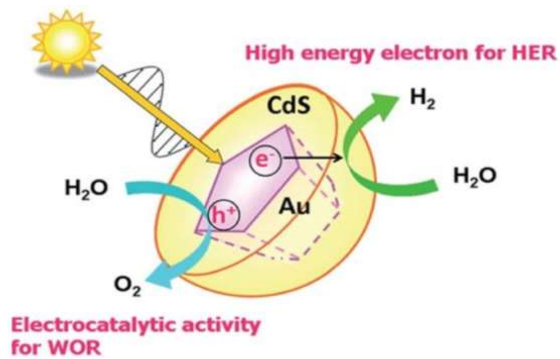

Figure 1.8 Schematic representation of photothermally boosted water splitting by the HCAu@#CdS/TiO_2 plasmonic photocatalyst.

However, integrating plasmonic and photothermal components into electrochemical systems presents several challenges. Stability under electrochemical and photo-induced conditions, especially for metals prone to oxidation such as Ag and Cu, remains a key limitation. Furthermore, the spatial and temporal control of local heating and charge injection is difficult to quantify and optimize. Advanced spectroscopic and operando techniques are being developed to probe the dynamic behavior of hot carriers, interfacial temperatures, and light-matter interactions at catalytic surfaces[36].

1.6 Organization of thesis

This thesis is organized into 3 chapters. Chapter 1 is an introduction to the electrochemical water splitting. Chapter 2 presents the nitridated $NiMoO_4$ catalyst for HER. Chapter 3 discusses the photo-thermal enhancement of Co_3Mo_3N for OER.

Chapter 2: Pt doped nitridated $NiMoO_4$ and its electrochemical performance in hydrogen evolution reaction (HER)

2.1 Introduction and inspiration

The global transition toward sustainable energy systems has renewed interest in hydrogen as a clean, carbon-free energy carrier. Among hydrogen production technologies, electrochemical water splitting stands out for its simplicity, scalability, and compatibility with renewable electricity. However, the widespread deployment of this technology is constrained by the reliance on precious metal catalysts, particularly platinum, which remains the benchmark for the HER due to its near-optimal hydrogen adsorption energy and outstanding kinetics. The high cost and scarcity of Pt, however, present significant barriers to commercial viability. As a result, the development of non-precious metal catalysts with comparable HER activity has become a pressing area of research in energy materials.

One promising class of alternatives is non-precious metal nitrides, such as molybdenum nitride (Mo_2N), nickel nitride (Ni_3N), cobalt nitride (Co_4N), and their bimetallic combinations. These materials offer favorable electronic properties, chemical stability in alkaline media, and metallic conductivity, all of which are advantageous for HER. Their partially filled d-bands can be tuned to optimize the hydrogen adsorption free energy, allowing them to effectively catalyze both the Volmer and Heyrovsky (or Tafel) steps of HER. In particular, bimetallic nitrides such as those derived from nickel and molybdenum precursors have shown synergistic effects combining the favorable hydrogen binding energy of Mo with the excellent electrical conductivity and surface reactivity of Ni. These properties make them ideal candidates for earth-abundant HER catalysts.

A key inspiration for this work comes from a study by Zhang et al.[37]. In that study, the authors synthesized hierarchical $MoNi_4$, or reduced $NiMoO_4$ nanostructures on nickel foam through a hydrothermal method. The resulting architecture exhibited excellent pseudocapacitive performance due to its high surface area, porous morphology, and abundant redox-active sites.

While the primary application in that work was energy storage, the unique structural and compositional features of $NiMoO_4$ made it a compelling candidate for catalytic reactions such as HER.

However, a major limitation observed was the chemical instability of the hydrated $MoNi_4$ phase. When exposed to air, the highly active $MoNi_4$ rapidly reacts with oxygen and moisture, leading to structural degradation and loss of function. This issue poses a significant barrier to real-world deployment, where ambient stability is critical. Motivated by this challenge, the present work introduces a strategic modification in the synthesis step, which is nitridation. This approach avoids the formation of air-sensitive $MoNi_4$ nanostructure into a stable, conductive nitride form while retaining its advantageous morphology. The resulting nitridated $NiMoO_4$ is expected to inherit both the structural benefits of the parent oxide and the catalytic performance advantages of transition metal nitrides.

The nitridation offers several key advantages, including higher electrical conductivity than oxides, increased stability under both air and electrochemical conditions, formation of heterostructures and defects that create abundant active sites for hydrogen adsorption, and enhanced hydrogen adsorption/desorption kinetics, owing to optimized electronic structures. Together, these factors result in a material with significantly improved HER activity and durability. In alkaline electrolytes, where water dissociation is a critical step, nitridated $NiMoO_4$ can promote both the Volmer step and subsequent hydrogen evolution steps effectively[38].

In the course of this research, it was found that depositing a small amount of platinum into the nitridated $NiMoO_4$ catalyst led to a remarkable enhancement in HER performance. Specifically, the Pt-doped nitridated $NiMoO_4$ exhibited a much higher current density at low overpotential compared to the undoped material. This enhancement is attributed to the synergistic effect between Pt and the nitride host matrix. The small amount of Pt likely introduces highly active hydrogen adsorption sites, mimicking the behavior of pure Pt catalysts, improved electronic coupling between the nitride substrate and surface intermediates, and stronger water dissociation capability, especially important under alkaline conditions.

Notably, the catalyst reached a current density of 350 mA cm^{-2} at only -10 mV overpotential when Pt was introduced, outperforming most reported Ni-Mo-based catalysts. This suggests that trace amounts of noble metals, when strategically incorporated, can significantly enhance the activity of non-precious metal systems while minimizing cost. These findings open new directions in HER catalyst design, where hybrid systems combining non-precious backbones with ultra-low-loadings of PGMs may offer the best of both worlds.

While the main objective of this thesis is to explore and validate non-precious metal nitride-based catalysts, the observed enhancement via Pt doping highlights the importance of interface engineering and atomic-level tuning in HER catalysis. Moving forward, the challenge will be to replace Pt entirely by identifying dopants or co-catalysts that offer similar benefits, such as transition metal phosphides, carbides, or single-atom catalysts with earth-abundant elements.

In summary, nitridated $NiMoO_4$ provides a highly promising platform for HER catalysis. Its performance can be further enhanced through targeted doping, as demonstrated by Pt incorporation. These results position this material as a strong candidate for future development in affordable, efficient hydrogen production systems.

2.2 Experimental section

Preparation of $NiMoO_4$ nanorods on nickel foam. $NiMoO_4$ nanorods were prepared by following the procedure reported by Zhang et al[37]. In a typical synthesis, 15 mL of aqueous precursor solution containing 0.04 M nickel nitrate hexahydrate ($Ni(NO_3)_2 \cdot 6H_2O$) and 0.01 M ammonium molybdate tetrahydrate ($(NH_4)_6Mo_7O_{24} \cdot 4H_2O$) was prepared under constant stirring until fully dissolved. A piece of pre-cleaned Ni foam (1×3 cm^2) was immersed in the solution and transferred into a 25 mL Teflon-lined stainless-steel autoclave. The sealed autoclave was heated at 200 °C for 6 h and then allowed to cool naturally to room temperature. The resulting yellowish $NiMoO_4$-coated Ni foam (denoted $NiMoO_4$@NF) was thoroughly rinsed with deionized water and ethanol, and dried at 60 °C overnight under vacuum.

Reduction and nitridation of $NiMoO_4$@NF. The reduced and nitridated $NiMoO_4$ catalysts were synthesized by calcining the as-synthesized $NiMoO_4$ nanorods in a H_2/Ar (v/v, 5/95) atmosphere at 500 °C for 2 h and in NH_3 atmosphere at 600 °C for 2 h, respectively. To make a comparation, the $NiMoO_4$ precursor was also calcined in NH_3 atmosphere at different temperature.

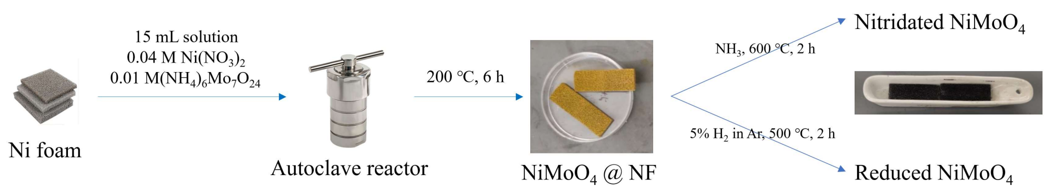

Figure 2.1 Synthesis of nitridated and reduced $NiMoO_4$ on nickel foam

Doping of platinum on $NiMoO_4$@NF and electrochemical test of HER. Platinum is doped onto the $NiMoO_4$@NF during the electrochemical test including cyclic voltammetry (CV) and chronoamperometry (CA). CV and CA were performed in a three-electrode configuration in a 1 M KOH aqueous solution using a Hg/HgO electrode and a Pt wire as the reference and counter electrodes, respectively. All potentials were referenced to the reversible hydrogen electrode (RHE), and the ohmic potential drop loss from the electrolyte resistance has been subtracted. Pt is dissolved in the electrolyte and then deposited onto the surface of $NiMoO_4$@NF.

Characterization of structure. Scanning electron microscope (SEM) images were taken with a FEI XL30 SEM-FEG microscope (operating voltage, 10 kV).

2.3 Results and discussion

2.3.1 Structure and morphology of nitridated and reduced $NiMoO_4$ on nickel foam

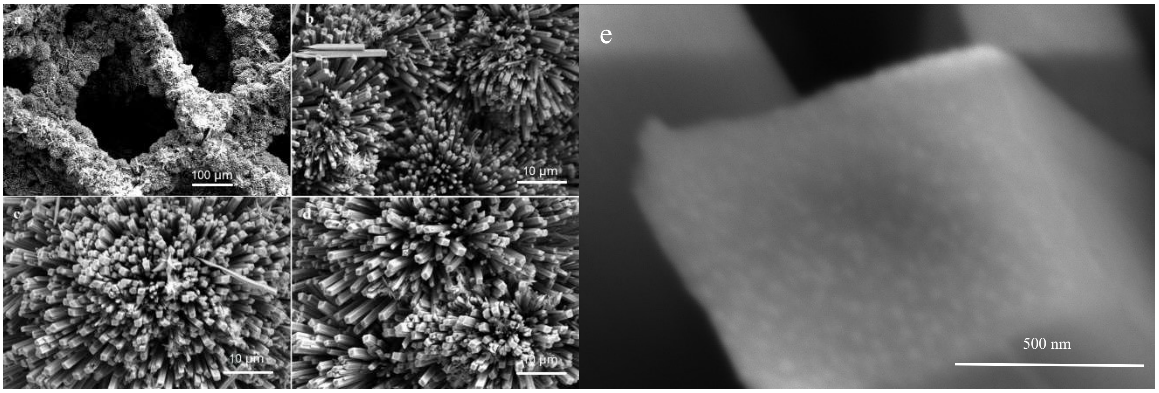

Figure 2.2 SEM images of (a)(b) $NiMoO_4$, (c)(e) nitridated $NiMoO_4$ and (d) reduced $NiMoO_4$.

Large area SEM image in Figure 2.2a shows sphere-like assemble of $NiMoO_4$ nanorods grown on Ni foam. The side length of $NiMoO_4$ nanorods is about 1 μm as shown in Figure 2.2b. $NiMoO_4$ nanorods preserve its structure even after NH_3 and H_2 calcination as seen in Figure 2.2c and 2.2d. Figure 2.2e shows nitridated $NiMoO_4$ nanoparticles on the $NiMoO_4$ nanorod substrate. The diameter of the nanoparticles is approximately 50 nm.

2.3.2 Deposition of platinum and its effect on HER

As shown in Figure 2.3a, nitridated $NiMoO_4$ displays superior HER activity compared to both reduced and plain $NiMoO_4$, characterized by a significantly higher cathodic current density at more positive potentials. Notably, the performance of nitridated $NiMoO_4$ even surpasses that of commercial Pt wire under identical conditions, suggesting an exceptional catalytic enhancement. However, further investigation in Figure 2.3b reveals that the observed high activity is closely linked to the choice of counter electrode. When Pt wire is used as the counter electrode, the HER current density of nitridated $NiMoO_4$ is markedly higher than when a carbon rod is used. This discrepancy indicates that Pt likely dissolves from the counter electrode during electrochemical testing and is subsequently redeposited onto the working electrode surface, effectively forming

Pt-decorated nitridated $NiMoO_4$, which is supported by the CA curve in Figure 2.4. The presence of Pt on the active surface introduces highly active hydrogen adsorption sites, thereby dramatically boosting HER performance. The result shows that Pt-decorated nitridated $NiMoO_4$ can serve as an efficient hybrid catalyst with synergistic activity from both Pt and metal nitrides.

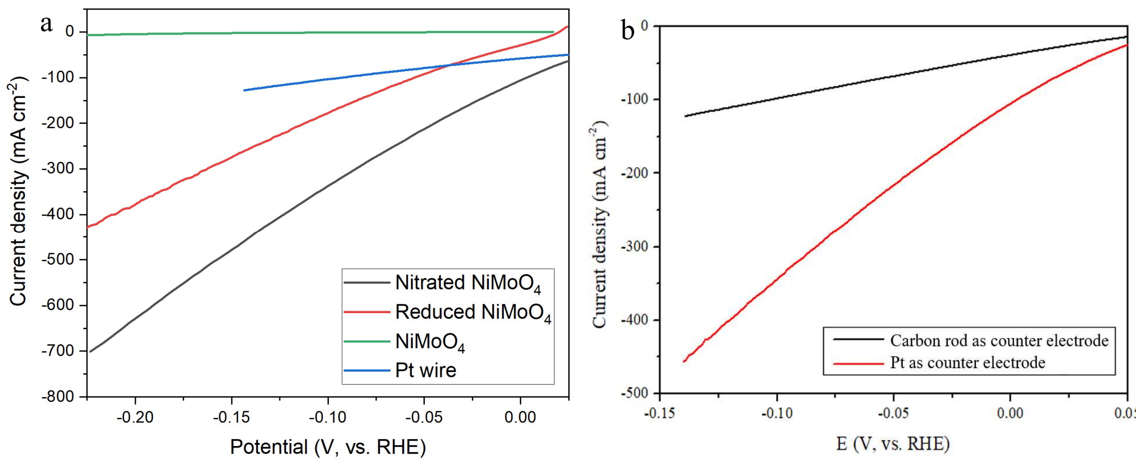

Figure 2.3 Performance of different catalyst for HER

(a) Part of CV of as-synthesized nitridated $NiMoO_4$, reduced $NiMoO_4$, plain $NiMoO_4$ on nickel foam and Pt wire in 1 M KOH solution with a Pt wire as counter electrode. (b) Part of CV of nitridated $NiMoO_4$ on nickel foam in 1 M KOH solution with different counter electrode.

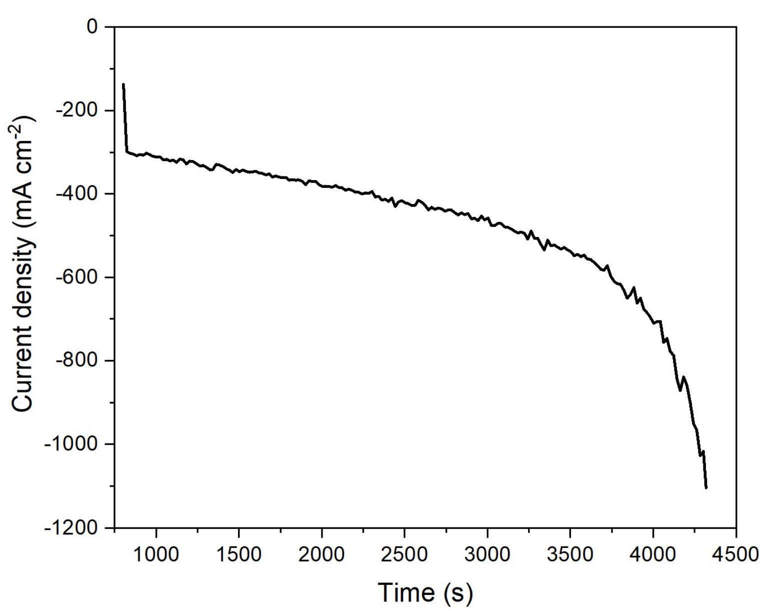

Figure 2.4 CA curve of the deposition of platinum on to nitridated $NiMoO_4$ on nickel foam in 1 M KOH at the potential of -0.3 V vs RHE

2.3.3 Effect of calcination temperature on the HER activity of nitridated $NiMoO_4$

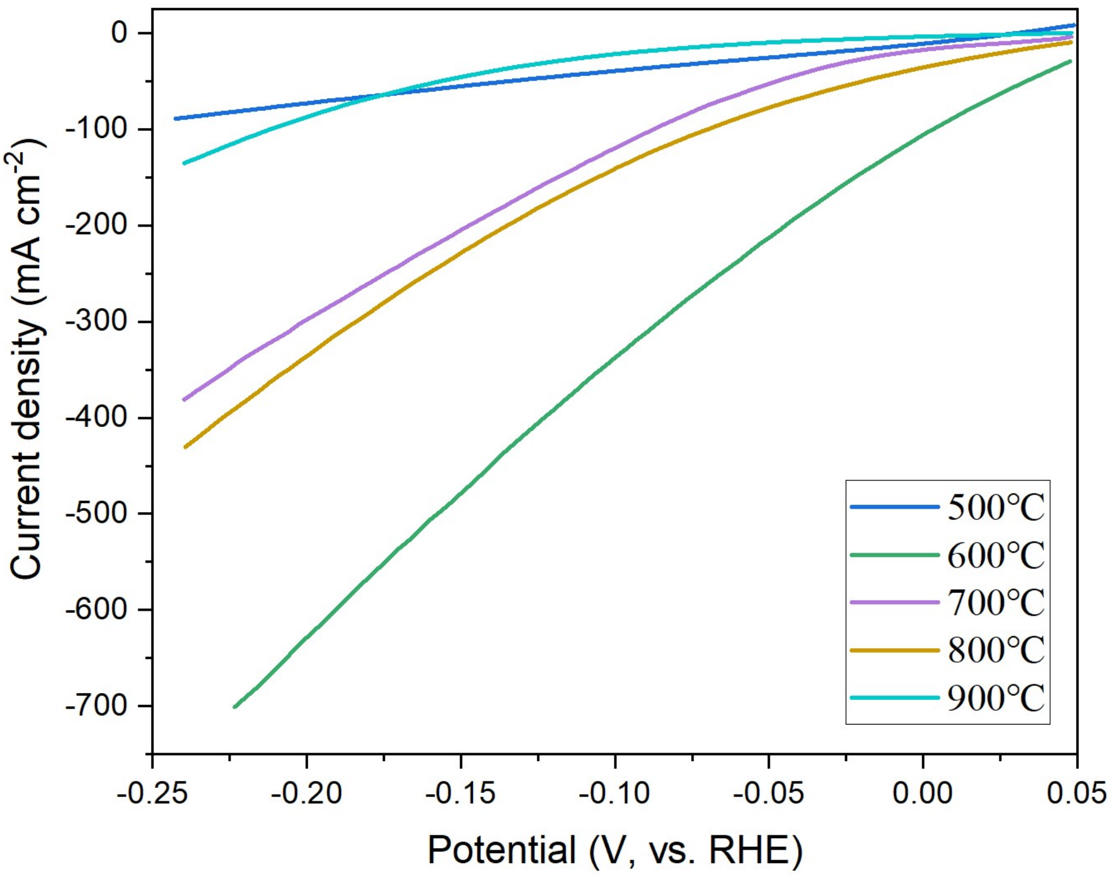

Figure 2.5 Comparation of nitridated $NiMoO_4$ on nickel foam calcined under different temperature

Figure 2.5 presents the CV curves of nitridated $NiMoO_4$ on nickel foam, calcined at various temperatures ranging from 500 °C to 900 °C under an ammonia atmosphere. The HER activity is strongly dependent on the calcination temperature, as reflected in the variation of current density with applied potential. The sample treated at 600 °C exhibits the highest catalytic performance, with the largest cathodic current density and most favorable onset potential, indicating optimal electronic conductivity and hydrogen adsorption kinetics. At lower temperatures, the incomplete nitridation and limited crystallinity likely hinder the formation of active sites and reduce electrical conductivity. Conversely, excessively high temperatures may lead to sintering or structural collapse of the nanorods, reducing the surface area and active site accessibility, thereby diminishing HER activity. These results demonstrate that 600 °C represents the optimal thermal treatment condition for enhancing the electrochemical performance of nitridated $NiMoO_4$, achieving a balance between crystalline quality, phase composition, and structural integrity.

2.3.4 Stability test

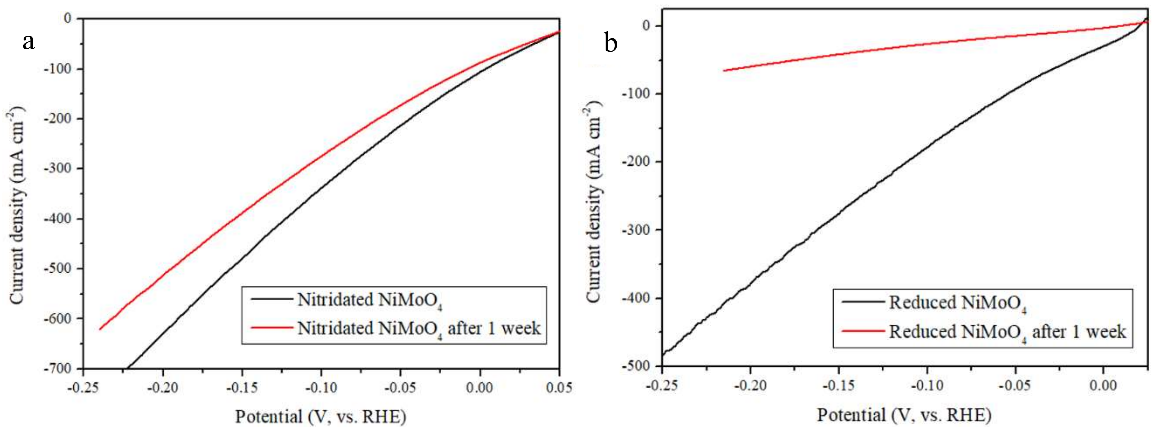

Figure 2.6 Stability comparison of nitridated and reduced $NiMoO_4$ catalysts for HER after one week of ambient storage

Figure 2.6 assesses the stability of both nitridated and reduced $NiMoO_4$ catalysts over the course of one week by comparing their HER performance before and after storage in air. As shown in panel (a), the nitridated $NiMoO_4$ sample demonstrates remarkable electrochemical durability, with its CV curve after one week (red) closely matching or even exceeding the initial performance (black). This suggests a possible activation effect upon exposure, or minimal degradation of the nitridated surface and active sites. In contrast, panel (b) shows that reduced $NiMoO_4$ suffers significant performance loss after one week, as evidenced by a dramatic decrease in cathodic current density. The decline in activity is likely due to oxidation or surface passivation in ambient air, indicating poor structural and chemical stability of the reduced phase. These results highlight the superior long-term robustness of nitridated $NiMoO_4$ for HER applications, making it a more viable candidate for practical alkaline electrolysis systems.

2.4 Conclusion

In summary, Pt-doped nitridated $NiMoO_4$ synthesized via ammonia treatment of hydrothermally grown $NiMoO_4$ nanorods on nickel foam exhibits outstanding electrocatalytic performance toward the HER in alkaline media. Systematic comparison with pristine and reduced $NiMoO_4$ demonstrates that nitridation significantly enhances catalytic activity, primarily due to improved electronic conductivity, increased active site availability, and optimized hydrogen adsorption energy. Among various post-treatment temperatures, 600 °C is identified as the optimal nitridation condition, balancing crystallinity and surface area to achieve the highest current density. Moreover, stability tests reveal that nitridated $NiMoO_4$ retains or even improves its activity after prolonged exposure to ambient air, unlike its reduced counterpart, which suffers significant degradation. The enhanced durability further underlines its potential for long-term alkaline water electrolysis. Future work will aim to build upon the success of nitridated $NiMoO_4$ by addressing several critical aspects for improving performance and practical applicability. One of the primary goals is the complete elimination of precious metals. Although platinum doping has shown a strong enhancement in HER activity, future studies will explore alternative dopants such as iron, cobalt, or even single-atom catalysts derived from earth-abundant elements to replicate the catalytic benefits without the associated cost. To better understand the reaction pathways and surface interactions, in situ and operando spectroscopic techniques, such as in situ X-ray photoelectron spectroscopy (XPS), Raman spectroscopy, or Fourier-transform infrared spectroscopy (FTIR) will be employed to track intermediate species during electrochemical operation. Further optimization will involve interface and defect engineering, including the modulation of nitrogen vacancies and strain within the nitride lattice to increase active site density and fine-tune hydrogen binding energetics. Additionally, inspired by the performance of Co_3Mo_3N in photo-thermal environments, the integration of nitridated $NiMoO_4$ into light-assisted HER systems will be explored to enhance activity under solar irradiation. Long-term electrochemical durability testing under industrially relevant conditions, as well as stability under ambient air exposure, will also be prioritized to ensure real-world viability. Finally, scalable synthesis methods and a preliminary techno-economic assessment will be undertaken to evaluate the potential of nitridated $NiMoO_4$-based systems for large-scale, low-cost green hydrogen production.

Chapter 3: Photo-thermal behavior of electrocatalyst Co_3Mo_3N in oxygen evolution reaction (OER)

3.1 Introduction and inspiration

The global transition toward carbon neutrality demands efficient, low-cost, and scalable technologies for renewable energy conversion and storage. Electrochemical water splitting is a cornerstone of this transition, offering a sustainable route to hydrogen production. However, the overall efficiency of water electrolysis remains constrained by the sluggish kinetics of the OER, which requires multistep proton-coupled electron transfer and the formation of O-O bonds. To address this bottleneck, there is intense interest in developing earth-abundant OER electrocatalysts that rival the performance of precious metals such as Ir and Ru.

Among the most promising alternatives are transition metal nitrides, especially bimetallic nitrides such as Co_3Mo_3N. This material exhibits excellent intrinsic OER activity, derived from the synergistic interaction between Co and Mo atoms, high electrical conductivity, and robust stability in alkaline conditions[38]. Prior studies have shown that Co_3Mo_3N features abundant active sites with favorable adsorption energies for oxygenated intermediates, enabling low overpotentials and Tafel slopes comparable to state-of-the-art catalysts[39].

Recent advances in plasmonic and photo-thermal electrocatalysis have opened a new frontier in catalyst design. While localized surface plasmon resonances (LSPRs) are typically associated with noble metals like Au and Ag, cobalt nanoparticles have also been shown to support LSPR-like behavior in the visible and near-infrared ranges[28]. Upon light excitation, these oscillations generate localized electromagnetic fields and rapid non-radiative decay, leading to localized heating, or photo-thermal effect[40]. This localized heat can modulate reaction kinetics, reduce activation barriers, and enhance catalytic rates via thermal activation of sluggish steps.

Inspired by these insights, we hypothesized that Co_3Mo_3N, with its plasmonic-like Co domains and metallic conductivity, could serve not only as a robust OER catalyst but also as an efficient photo-thermal catalyst under light irradiation. Preliminary experiments revealed a dramatic enhancement in OER current density upon exposure to visible light. Under 2 W blue LED illumination, Co_3Mo_3N exhibited a ~150% increase in current density at an overpotential of 0.34 V, alongside a reduced Tafel slope, indicating accelerated reaction kinetics.

While the plasmonic behavior of Co plays a central role, another critical factor contributing to this enhancement is the synergistic interaction between Co_3Mo_3N and the carbon paper support. Carbon paper not only serves as a conductive substrate but also participates actively in photo-thermal modulation. First, it absorbs a broad spectrum of light and efficiently converts it into heat, creating a localized temperature gradient at the catalyst-electrolyte interface. Second, the close contact between Co_3Mo_3N nanoparticles and the carbon surface promotes rapid electron transfer, facilitating charge separation and reducing ohmic resistance during OER operation[41]. This synergy results in enhanced light absorption, localized thermal confinement, and improved mass and charge transport, all of which contribute to the unusually high photo-thermal enhancement observed. The effect is particularly pronounced in Co_3Mo_3N compared to non-supported or oxide-based catalysts, where the lack of interfacial conductivity limits the thermal-to-electrochemical energy transfer. Furthermore, the carbon matrix may stabilize intermediate oxidation states of Co and Mo during operation, improving catalyst durability[42].

The demonstrated enhancement of Co_3Mo_3N under light irradiation highlights a new strategy for designing multifunctional electrocatalysts that respond synergistically to electrical, thermal, and optical stimuli. Instead of treating light merely as an energy input for photocatalysis, this approach leverages thermal modulation at the nanoscale to overcome kinetic limitations. The Co_3Mo_3N/carbon paper system offers a prototype platform where materials chemistry and photonic engineering converge to improve catalytic outcomes.

Ultimately, this work not only advances the fundamental understanding of photo-thermal electrocatalysis but also supports the practical development of solar-assisted water splitting technologies using abundant and durable materials.

3.2 Experimental section

Preparation of $CoMoO_4$ precursors. The $CoMoO_4$ precursor is prepared by following the procedure reported by Yuan et al[42]. In a typical synthesis, 50 mL of aqueous precursor solution containing 1.00 g cobalt chloride hexahydrate ($CoCl_2 \cdot 6H_2O$) and 1.02 g sodium molybdate ($Na_2MoO_4 \cdot 2H_2O$) was prepared under constant stirring until fully dissolved. The solution is then heated in water bath at 60 °C under magnetic agitation for 5 hours and a purple precipitate is obtained. After vacuum filtration, the precipitate is washed with distilled water and dried at 60 °C for 24 h.

Synthesis of Co_3Mo_3N. For nitridation via ammonolysis, 0.5 g of $CoMoO_4$ precursor is placed in a horizontal tube furnace and heated under a NH_3 flow (20 mL min^{-1}) at 800 °C for 1 h. After nitridation, the furnace is cooled down to room temperature naturally, and the black sample is passivated overnight in a flow of Ar mixture to prevent the oxidation when exposed in the atmosphere.

Electrochemical test of HER. Cyclic voltammetry (CV) and chronoamperometry (CA) were performed in a three-electrode configuration in a 1 M KOH aqueous solution using a Hg/HgO electrode and a carbon rod as the reference and counter electrodes, respectively. All potentials were referenced to the reversible hydrogen electrode (RHE), and the ohmic potential drop loss from the electrolyte resistance has been subtracted.

Characterization of structure. Scanning electron microscope (SEM) images were taken with a FEI XL30 SEM-FEG microscope (operating voltage, 10 kV).

3.3 Results and discussion

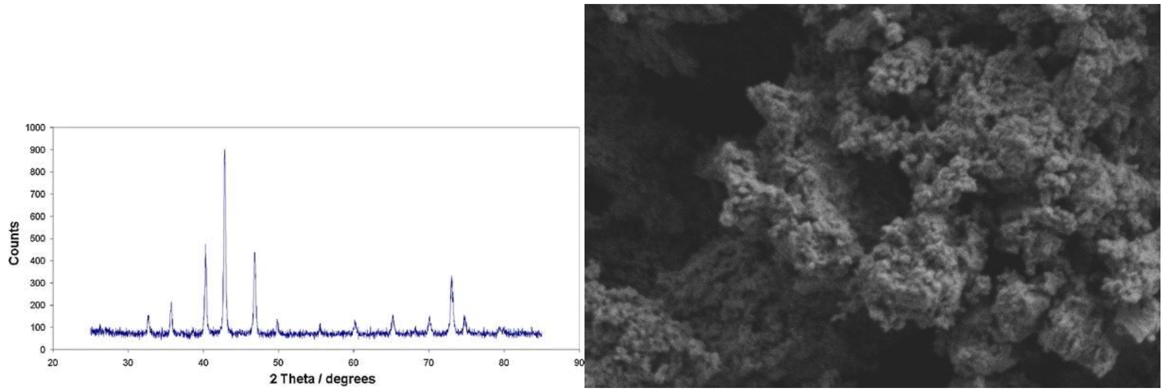

Figure 3.1 XRD and SEM images of Co_3Mo_3N.

XRD image in Figure 3.1 confirms the successful synthesis of Co_3Mo_3N, and SEM image in Figure 3.1 shows the morphology of Co_3Mo_3N nanoparticles on carbon paper. Figure 3.2 presents the CV curves of Co_3Mo_3N deposited on carbon paper and fluorine-doped tin oxide (FTO) glass, compared against commercial Pt/C catalyst on FTO, for OER in alkaline medium. Among the tested samples, Co_3Mo_3N on carbon paper exhibits a significantly higher current density over the entire voltage range, reaching over 45 mA cm^{-2} at 1.6 V vs. RHE. In contrast, Co_3Mo_3N on FTO glass and Pt/C on FTO show negligible current response until potentials above 1.55 V, indicating poor electrocatalytic activity under these conditions. This pronounced enhancement for Co_3Mo_3N on carbon paper highlights the critical role of the support material. Carbon paper not only provides superior electrical conductivity and interfacial contact but may also synergize with Co_3Mo_3N to enhance light absorption and local heating under photo-thermal conditions, consistent with prior observations of support-mediated effects. The result emphasizes the importance of rational electrode design, where both the intrinsic catalyst properties and the characteristics of the support material collectively influence the overall catalytic performance in OER.

Figure 3.3 shows a steady increase in current density over a 2-hour period under dark conditions with gradual heating. This trend confirms that the catalytic activity is strongly temperature-dependent, with a pronounced increase in current observed beyond 1.5 hours, suggesting enhanced electrochemical kinetics at elevated temperatures. While no light was applied in this experiment, the significant thermal response indicates that the catalyst is heat-sensitive and capable of thermally driven catalytic enhancement.

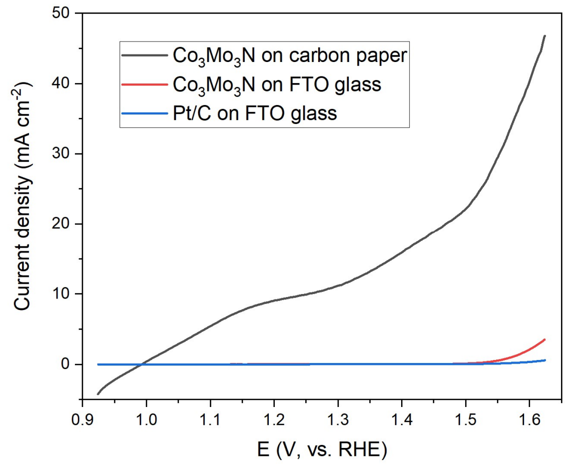

Figure 3.2 Comparison of OER performance of Co_3Mo_3N on carbon paper and FTO glass with benchmark Pt/C catalyst

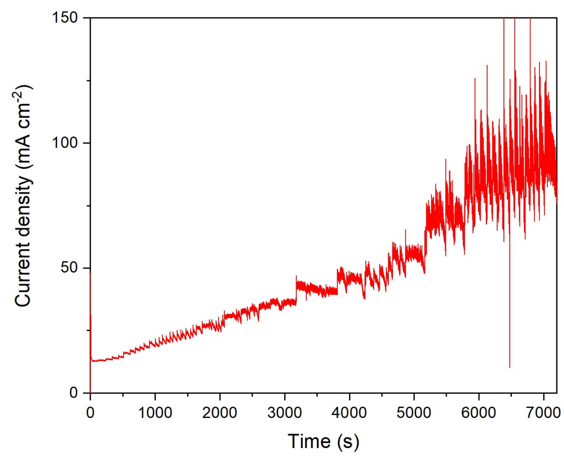

Figure 3.3 CA response of Co_3Mo_3N electrocatalyst under gradual heating in dark condition

The temperature increases from room temperature at the beginning to 45 °C in the end.

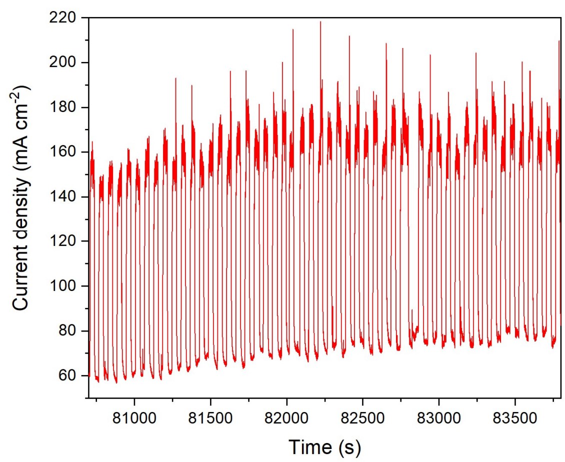

Figure 3.4 CA curve of Co_3Mo_3N electrocatalyst on carbon paper in 1 M KOH aqueous solution at 1.57 V vs. RHE alternating the on/off of blue light.

Figure 3.4 shown exhibits sharp, periodic current density spikes corresponding to the on/off cycles of blue light irradiation at a constant potential of 1.57 V vs. RHE. Notably, during each light-on period, the current density rapidly rises from a baseline of approximately 60-80 mA cm^{-2} to peaks exceeding 140-170 mA cm^{-2}, representing an approximately 250% enhancement in electrocatalytic activity. When considered alongside previous heating-under-dark-condition data, these results provide compelling evidence that the electrocatalyst functions via a photo-thermal mechanism. This dramatic increase confirms the photo-thermal electrocatalytic behavior of the Co_3Mo_3N catalyst, where incident light contributes to local heating effects, reducing kinetic and charge transfer barriers at the interface. Moreover, the response is highly reversible and stable over many cycles, indicating not only a robust and repeatable photo-thermal effect but also the chemical and structural stability of the catalyst under operational conditions. The gradual increase in base current over time further suggests a cumulative light-induced activation or possible surface restructuring that favors enhanced OER kinetics.

These findings place Co_3Mo_3N among the most promising non-precious metal-based photo-thermal OER catalysts, demonstrating its viability for integration into solar-driven water-splitting devices. The magnitude of the enhancement highlights the importance of light-catalyst interactions in designing future catalysts that can fully leverage solar energy in electrochemical systems.

3.4 Conclusion

In this study, Co_3Mo_3N nanoparticles supported on carbon paper were synthesized and evaluated as photo-thermal electrocatalysts for OER in alkaline media. The catalyst exhibited pronounced activity enhancements under both light and thermal stimuli, as confirmed by chronoamperometric measurements under periodic blue light irradiation and gradual heating under dark condition. Specifically, the catalyst showed rapid and reversible current responses to light on/off cycles, and a substantial increase in current density at elevated temperatures, confirming its photo-thermal responsiveness. These characteristics indicate efficient thermal activation behavior, highlighting the potential of Co_3Mo_3N for integration into solar-assisted water-splitting systems. Importantly, the performance was achieved without the use of precious metals, underscoring the viability of Co_3Mo_3N as a cost-effective and sustainable OER catalyst. Future work should explore optimizing the nanostructure and exploring scalable synthesis strategies to further enhance light-heat synergy and long-term operational stability in real-world solar electrolyzer environments.

Moving forward, this project aims to explore several key directions to further advance the performance of Co_3Mo_3N-based photo-thermal electrocatalysts. Efforts will focus on tuning the particle-support interface to optimize light absorption and thermal confinement at the catalyst surface. In parallel, nanostructuring strategies will be investigated to enhance light-matter interactions and increase active surface area. This approach will also be expanded to other transition metal-based systems with plasmonic potential, broadening the design space for multifunctional catalysts. Finally, long-term operational stability under continuous light irradiation and diverse electrolyte conditions will be systematically evaluated to assess the practical viability of these materials for solar-assisted water splitting applications.

Chapter 4: Conclusions

In this dissertation, the development of non-precious metal nitrides has been systematically investigated for efficient electrochemical water splitting, with particular attention to hydrogen evolution reaction (HER) and oxygen evolution reaction (OER) in alkaline environments. Through the rational design and synthesis of nanostructured catalysts, nitridated $NiMoO_4$ for HER and photo-thermally enhanced Co_3Mo_3N for OER, this work highlights the importance of surface chemistry, electronic configuration, and material-support synergy in boosting catalytic performance. The findings underscore how morphological control, interfacial engineering, and even light-induced thermal modulation can together enhance the activity and durability of earth-abundant electrocatalysts.

Future research will expand upon these results by integrating advanced compositional strategies and operando analysis tools. One key direction is the development of multi-metal nitrides, such as high-entropy nitrides incorporating five or more transition metals, which offer a tunable landscape of active sites and defect structures. These could be synthesized via modified hydrothermal ammonolysis or ball-milling nitridation methods. Their surface chemistry, electronic states, and nitrogen vacancy concentrations will be systematically probed using a suite of characterization tools including XPS, EPR, UPS, XRD, and TEM.

Simultaneously, the photo-thermal catalytic concept demonstrated in Co_3Mo_3N will be expanded to non-noble metal systems, and nanostructuring techniques will be employed to enhance light absorption and thermal localization. Carbon-based supports and 2D conductive substrates will be explored to reinforce interfacial charge transfer. Meanwhile, strategies to eliminate the use of Pt as a counter electrode will be prioritized to achieve completely noble-metal-free electrolyzers.

Another important avenue is the implementation of light-assisted water-splitting devices, where catalyst-photon coupling, temperature response, and electrolyte interface behavior can be studied under controlled illumination. Operando techniques such as in situ Raman, FTIR, or XAS will provide mechanistic insights into intermediate formation, surface reconstructions, and electronic transitions during real-time catalysis.

Ultimately, the goal is to establish a generalizable framework for designing scalable, stable, and solar-integrated electrochemical systems that can convert intermittent renewable energy into hydrogen fuel. By advancing our understanding of composition-structure-function relationships in transition metal nitrides and incorporating photonic strategies, this work lays the foundation for the next generation of affordable, high-efficiency water splitting technologies.

References

1. BP. Statistical Review of World Energy, 2023.

2. International Energy Agency (IEA). CO_2 Emissions in 2022, IEA Publications, **2023**.

3. IPCC. Climate Change 2021: The Physical Science Basis, Working Group I Contribution to the Sixth Assessment Report.

4. Klare, M. T. The Race for What's Left: The Global Scramble for the World's Last Resources, Metropolitan Books, **2012**.

5. IEA. World Energy Outlook, **2022**.

6. Eaton, D. W. Global Energy Sources. EARTH 104: Earth and the Environment, Penn State University.

7. Halkos, G. E.; Gkampoura, E.-C. Reviewing Usage, Potentials, and Limitations of Renewable Energy Sources. *Energies* **2020**, *13* (11), 2906.

8. IRENA. Renewable Power Generation Costs in 2022, International Renewable Energy Agency, **2023**.

9. Bicer, Y.; Dincer, I.; Vezina, G.; Raso, F. Impact Assessment and Environmental Evaluation of Various Ammonia Production Processes. *Environ. Manage.* **2017**, *59*, 842-855.

10. Seh, Z. W.; Kibsgaard, J.; Dickens, C. F.; Chorkendorff, I.; Nørskov, J. K.; Jaramillo, T. F. Combining theory and experiment in electrocatalysis: Insights into materials design *Science* **2017**, *355*, eaad4998.

11. Dincer, I.; Acar, C. Review and evaluation of hydrogen production methods for better sustainability *Int. J. Hydrogen Energy* **2015**, *40*, 11094-11111.

12. IRENA. Green Hydrogen: A Guide to Policy Making, International Renewable Energy Agency, **2020**.

13. Berkeley Lab. Hydrogen: The Energy Carrier of the Future; Energy Technologies Area, Lawrence Berkeley National Laboratory: **2020**.

14. Łosiewicz, B. Technology for Green Hydrogen Production: Desk Analysis. *Energies* **2024**, *17* (17), 4514.

15. European Commission. A Hydrogen Strategy for a Climate-Neutral Europe, **2020**.

16. Roger, I.; Shipman, M. A.; Symes, M. D. Earth-Abundant Catalysts for Electrochemical and Photoelectrochemical Water Splitting. *Nat. Rev. Chem.* **2017**, *1* (1), 0003.

17. Zeng, K.; Zhang, D. Recent Progress in Alkaline Water Electrolysis for Hydrogen Production and Applications. *Prog. Energy Combust. Sci.* **2010**, *36* (3), 307-326.

18. Conway, B. E.; Tilak, B. V. Interfacial Processes Involving Electrocatalytic Evolution and Oxidation of H_2, and the Role of Chemisorbed Hydrogen. *Electrochim. Acta* **2002**, *47* (22-23), 3571-3594.

19. Sheng, W.; Myint, M.; Chen, J. G.; Yan, Y. Correlating the Hydrogen Evolution Reaction Activity in Alkaline Electrolytes with the Hydrogen Binding Energy on Monometallic Surfaces. *Energy Environ. Sci.* **2013**, *6*, 1509-1512.

20. McCrory, C. C. L.; Jung, S.; Peters, J. C.; Jaramillo, T. F. Benchmarking Heterogeneous Electrocatalysts for the Oxygen Evolution Reaction. *J. Am. Chem. Soc.* **2013**, *135* (45), 16977-16987.

21. Zhang, F.; Zhou, J.; Chen, X.; Zhao, S.; Zhao, Y.; Tang, Y.; Tian, Z.; Yang, Q.; Slavcheva, E.; Lin, Y.; Zhang, Q. The Recent Progresses of Electrodes and Electrolysers for Seawater Electrolysis. *Nanomaterials* **2024**, *14* (3), 239.

22. Ďurovič, M.; Hnát, J.; Bouzek, K. Electrocatalysts for the Hydrogen Evolution Reaction in Alkaline and Neutral Media. A Comparative Review. *J. Power Sources* **2021**, *493*, 229708.

23. Gong, M.; Dai, H. A Mini Review of NiFe-Based Materials as Highly Active Oxygen Evolution Reaction Electrocatalysts. *Nano Res*. **2014**, *8*, 23-39.

24. Bockris, J. O'M.; Otagawa, T. Mechanism of Oxygen Evolution on Perovskites. *J. Phys. Chem.* **1983**, *87* (15), 2960-2971.

25. Voiry, D.; Salehi, M.; Silva, R.; Fujita, T.; Chen, M.; Asefa, T.; Shenoy, V. B.; Eda, G.; Chhowalla, M. Conducting MoS_2 Nanosheets as Catalysts for Hydrogen Evolution Reaction. *Nano Lett.* **2013**, *13* (12), 6222-6227.

26. Calle-Vallejo, F.; Díaz-Morales, O. A.; Kolb, M. J.; Koper, M. T. M. Why Is Bulk Thermochemistry a Good Descriptor for the Electrocatalytic Activity of Transition Metal Oxides? *ACS Catal.* **2015**, *5* (2), 869-873.

27. Jia, Y.; Zhang, L.; Du, A.; Gao, G.; Chen, J.; Yan, X.; Brown, C. L.; Yao, X. Defect Graphene as a Trifunctional Catalyst for Electrochemical Reactions. *Adv. Mater.* **2016**, *28* (43), 9532-9538.

28. Clavero, C. Plasmon-Induced Hot-Electron Generation at Nanoparticle/Metal-Oxide Interfaces for Photovoltaic and Photocatalytic Devices. *Nat. Photonics* **2014**, *8,* 95-103.

29. Zhang, Y.; He, S.; Guo, W.; Hu, Y.; Huang, J.; Mulcahy, J. R.; Wei, W. D. Surface-Plasmon-Driven Hot Electron Photochemistry. *Chem. Rev.* **2018**, *118* (6), 2927-2954.

30. Li, M.; Zhu, Y.; Wang, H.; Wang, C.; Pinna, N.; Lu, X. Ni Strongly Coupled with Mo_2C Encapsulated in Nitrogen-Doped Carbon Nanofibers as Robust Bifunctional Catalyst for Overall Water Splitting. *Adv. Energy Mater.* **2019**, *9* (10), 1803185.

31. Ai, L.; Su, J.; Wang, M.; Jiang, J. Bamboo-Structured Nitrogen-Doped Carbon Nanotube Coencapsulating Cobalt and Molybdenum Carbide Nanoparticles: An Efficient Bifunctional Electrocatalyst for Overall Water Splitting. *ACS Sustainable Chem. Eng.* **2018**, *6* (8), 10017-10026.

32. Wei, Y.; Li, W.; Li, D.; Yi, L.; Hu, W**.** Amorphous-Crystalline Cobalt-Molybdenum Bimetallic Phosphide Heterostructured Nanosheets as Janus Electrocatalyst for Efficient Water Splitting. *Int. J. Hydrogen Energy* **2022**, *47* (12), 7783-7792.

33. Li, X.; Bi, W.; Zhang, L.; Tao, S.; Chu, W.; Zhang, Q.; Luo, Y.; Wu, C.; Xie, Y. Single-Atom Pt as Co-Catalyst for Enhanced Photocatalytic H_2 Evolution. *Adv. Mater.* **2016**, *28* (12), 2427-2431.

34. J.Dey, A.; Mendalz, A.; Wach, A.; Bericat Vadell, R.; Silveira, V. R.; Leidinger, P. M.; Huthwelker, T.; Shtender, V.; Novotny, Z.; Artiglia, L.; Sá, J. Hydrogen Evolution with Hot Electrons on a Plasmonic-Molecular Catalyst Hybrid System. *Nat. Commun.* **2024**, *15*, 445.

35. Tada, H. Overall Water Splitting and Hydrogen Peroxide Synthesis by Gold Nanoparticle-Based Plasmonic Photocatalysts. *Nanoscale Adv.* **2019**, *1* (11), 4238-4245.

36. Zhang, J.; Wang, T.; Liu, P.; Liao, Z.; Liu, S.; Zhuang, X.; Chen, M.; Zschech, E.; Feng, X. Efficient hydrogen production on $MoNi_4$ electrocatalysts with fast water dissociation kinetics. *Nat. Commun.* **2017**, *8,* 15437.

37. Liang, H.-W.; Brüller, S.; Dong, R.; Zhang, J.; Feng, X.; Müllen, K. Molecular Metal-N_x Centres in Porous Carbon for Electrocatalytic Hydrogen Evolution. *Nat. Commun.* **2015**, *6*, 7992.

38. Liu, X.; Guo, Y.; Wang, P.; Wu, Q.; Zhang, Q.; Rozhkova, E. A.; Wang, Z.; Liu, Y.; Zheng, Z.; Dai, Y.; Huang, B. Synthesis of Synergistic Nitrogen-Doped $NiMoO_4/Ni_3N$ Heterostructure for Implementation of an Efficient Alkaline Electrocatalytic Hydrogen Evolution Reaction. *ACS Appl. Energy Mater.* **2020**, *3* (3), 2440-2449.

39. Christopher, P.; Xin, H.; Linic, S. Visible-Light-Enhanced Catalytic Oxidation Reactions on Plasmonic Silver Nanostructures. *Nat. Chem.* **2011**, *3,* 467-472.

40. Zhou, L.; Tan, Y.; Wang, J.; Xu, W.; Yuan, Y.; Cai, W.; Zhu, S.; Zhu, J. 3D Self-Assembly of Aluminum Nanoparticles for Plasmon-Enhanced Solar Desalination. *Nat. Photonics* **2016**, *10*, 393-398.

41. Mohana, P.; Yuvakkumar, R.; Ravi, G.; Arun, A.; Metha, S. A.; Dhanasekaran, P. A Porous Co_3Mo_3N/N-Doped Carbon Electrocatalyst Derived from Mo-Co MOFs for the Electrochemical Hydrogen Evolution Reaction. *New J. Chem.* **2024**, *48*, 20280-20295.

42. Yuan, Y.; Adimi, S.; Thomas, T.; Wang, J.; Guo, H.; Chen, J.; Attfield, J. P.; DiSalvo, F. J.; Yang, M. Co_3Mo_3N-An Efficient Multifunctional Electrocatalyst. *Innovation* **2021**, *2* (2), 100096.